ELSEVIER

Journal of Molecular Structure (Theochem) 591 (2002) 245–253

THEO CHEM

www.elsevier.com/locate/theochem

Collisional broadening and shifting of Raman lines, and the potential energy surface for H_2-Ar☆

Levi Waldron[a,b], Wing-Ki Liu[a,c,*], Robert J. Le Roy[a,c]

[a]*Department of Physics and Guelph-Waterloo Physics Institute, University of Waterloo, Waterloo, Ont., Canada N2L 3G1*
[b]*Faculty of Forestry, University of Toronto, 33 Willcocks Street, Toronto, Ont., Canada M5S 3B3*
[c]*Guelph-Waterloo Centre for Graduate Work in Chemistry and Biochemistry, University of Waterloo, Waterloo, Ont., Canada N2L 3G1*

Received 15 February 2002; revised 19 March 2002; accepted 26 March 2002

Abstract

Quantum mechanical close-coupling calculations of pressure broadened and pressure shifting coefficients for polarized vibrational Raman $Q_1(j)$ and pure rotational $S_0(j)$ Raman transitions of H_2-Ar and D_2-Ar have been performed using the empirically determined three-dimensional 'XC(fit)' potential energy surface. While the calculated $Q_1(j)$ vibrational line shifting coefficients, and both the shifting and broadening coefficients for the pure rotational $S_0(j)$ lines agree well with experiment, broadening coefficients calculated for the $Q_1(j)$ transitions are substantially smaller than the measured values. Test calculations using ad hoc modifications of the XC(fit) potential indicate that the diatom stretching dependence of that potential energy surface needs further refinement.

Keywords: Potential energy surface; H_2-Ar dimer; Collision broadening

1. Introduction

The analysis of spectral line shapes of molecular gases in the high density (pressure broadening) regime has long been recognized as a useful source of information about intermolecular forces [1,2]. With advances in coherent Raman spectroscopy [3–11], accurate measurements have been made of the line broadening, shifting, and mixing parameters for Raman transitions of molecular hydrogen isotopomers. In particular, line broadening and line shifting coefficients have been obtained for the polarized $Q_1(1)$ line of H_2-Ar over an extended range of temperature [4,8], and for the $Q_1(j)$ lines of D_2-Ar at room temperature [3,6]. The present paper uses these data to access the quality of the recently proposed 'XC(fit)' potential energy surface for the H_2-Ar system [12].

At moderately high gas density, the shape of an isolated Raman line is Lorentzian, and the broadening and shifting parameters can be obtained from the real and imaginary parts of a complex cross section which can be computed from a given intermolecular potential by solving a set of closed-coupled equations for the radial wave functions [1,2]. At higher gas

☆ We are pleased to dedicate this paper to Professor William J. Meath.

* Corresponding author. Address: Department of Physics and Guelph-Waterloo Physics Institute (G/W), University of Waterloo, Waterloo, Ont., Canada N2L 3G1. Tel.: +1-519-888-4567; fax: +1-519-746-8115.
E-mail address: wkliu@uwaterloo.ca (W.K. Liu).

0166-1280/02/$ - see front matter
PII: S0166-1280(02)00245-2

densities, different spectral lines begin to overlap, resulting in non-Lorentzian profiles whose asymmetric line shape can be described by a set of line-mixing parameters, which can again be obtained from a close-coupled scattering calculation. For the H_2–He system an accurate ab initio intermolecular potential is available [13], and within the Born–Oppenheimer approximation, the same potential governs the interaction between D_2 and He. Using this potential, quantum mechanical close-coupled calculation of the line broadening, line shifting and line-mixing parameters have been reported for the Raman $Q_1(j)$ lines [14–17]. Excellent agreement with experiment was found for both the pressure broadening and pressure shifting of the polarized $Q_1(j)$ lines. While no experimental data is available for the line-mixing parameters of the polarized spectrum or for any spectral parameter of the depolarized lines for D_2–He to compare with the theoretical calculations, this clearly demonstrates the high quality of that [13] ab initio potential.

Analogous close-coupled calculations of the pressure broadening and shifting of the $Q_1(j)$ lines of D_2–Ar were carried out by Green [18], employing an empirical potential energy surface determined by Le Roy and Hutson referred to as the 'TT_3' potential [19]. He found discrepancies with experiment of 20–40% for the line broadening (except for excellent agreement for the $j = 0$ line, which may be accidental), and of about 40% for the line shifts. The TT_3 potential had been determined from fits to discrete infrared spectra together with some data for collisional phenomena, including second virial coefficients and inelastic scattering cross sections. It was shown to be consistent with other scattering data, including total differential cross sections, thermal conductivity, and shear viscosity [19], although close-coupled calculations by Hutson [19] showed some discrepancy with experiment for pure rotational Raman linewidths and depolarized Rayleigh scattering cross sections, especially at low temperatures. Green suggested that this pointed to an inaccuracy in the vibrational dependence of the isotropic part of the potential at short range, which was not sufficiently sampled by the data used in its determination.

The more recent XC(fit) potential [12] was developed using the exchange-Coulomb model which was originally developed to describe the interactions of closed shell atoms [21–23], and the adjustable parameters in this model were determined by fitting to high resolution discrete infrared data and second virial coefficients. As expected, the XC(fit) potential proved as effective as the TT_3 potential for predictions of the spectroscopic and bulk data used in the fits to determine both potentials, but with improved accuracy due to the higher resolution and greater extent of the data used in its determination. In addition, the XC(fit) surface proved equally capable of predicting elastic and rotationally inelastic differential cross sections, as well as the hyperfine transition frequencies which had been used in the fits to determine the TT_3 potential, but not in those determining the XC(fit) potential. Furthermore, the XC(fit) potential was found to give fairly good agreement with experimental NMR spin–lattice relaxation times, especially at high temperatures ($T \gtrsim 400$ K) [24].

In an earlier paper [25] we attempted to assess the predictive ability of the XC(fit) potential for the vibrational Raman line broadening and shifting of D_2 in Ar. Our close-coupled calculation of the shifting coefficients for the $Q_1(j)$ lines for $j = 0$–5 were in good agreement with experiment. However, the predictions for the line broadening were less satisfactory. Although the j-dependence of the experimental broadening coefficients was qualitatively reproduced, the computed values were consistently smaller than the experimental ones. The present paper extends that work by examining the Raman line broadening and shifting coefficients for the H_2–Ar system in greater detail, in an attempt to delineate the deficiencies of the XC(fit) potential. Section 2 describes our application of the close-coupled scattering calculation method for computing the line broadening and shifting coefficients, while Section 3 presents our application of this method in predictions of the polarized Raman $Q_1(1)$ line of H_2–Ar. The broadening and shifting coefficient calculations for the pure rotational Raman $S_0(j)$ lines are reported in Section 4. Section 5 then describes calculations performed with modifications of the XC(fit) potential in an attempt to determine which parts of the potential function the width and shift parameter are most sensitive to, and our conclusions are presented in Section 6.

2. Scattering calculations

The theoretical expressions which relate the intermolecular potential to the line shape parameters, as well as the computational procedures for implementing them, were discussed previously [25]. The central object of the close-coupled scattering calculation is the complex cross section [1]

$$\sigma^{(\kappa)}_{f'i',fi}(E_k) = \frac{\pi}{k^2}\left(\frac{2j'_i+1}{2j_i+1}\right)^{1/2}\sum_{J_iJ_fll'}(-1)^{j_f-j'_f+l-l'} \times(2J_i+1)(2J_f+1)\begin{Bmatrix} j'_f & j'_i & \kappa \\ J_i & J_f & l' \end{Bmatrix}\begin{Bmatrix} j_f & j_i & \kappa \\ J_i & J_f & l \end{Bmatrix} \times\Big[\delta_{i'i}\delta_{f'f}\delta_{l'l} - S^{J_f}_{v'_fj'_fl',v_fj_fl}(E_k+E_{v_fj_f}) \times S^{J_i*}_{v'_ij'_il',v_ij_il}(E_k+E_{v_ij_i})\Big] \quad (1)$$

which depends on the scattering matrix element $S^J_{v'j'l',vjl}(E_k+E_{vj})$ that couples the system with initial vibration–rotation state (v,j), orbital and total angular momentum quantum numbers l, J, initial translational energy E_k and internal energy E_{vj}, to the final state (v',j',l',J). In Eq. (1), $i \equiv (v_i,j_i)$ and $f \equiv (v_f,j_f)$ refer to the initial and final spectroscopic states of the diatom before the collision, $i\!\setminus\!'$ and $f\!\setminus\!'$ to the corresponding states after collision, and κ is the tensorial rank of the multipole moment responsible for the spectral transition. For the polarized (isotropic) Raman spectrum, $\kappa = 0$, while $\kappa = 2$ for the depolarized Raman spectrum.

For an isolated $Q_1(j)$ Raman line, $v_i = 0$, $v_f = 1$, and $j_i = j_f = j$, while for the pure rotational Raman $S_0(j)$ line, $v_i = v_f = 0$, $j_i = j$ and $j_f = j+2$. The line shifting and broadening coefficients of an isolated spectral line $i \rightarrow f$ are given by the imaginary and real parts of the thermal average of the diagonal complex cross section, respectively [2],

$$\delta_{fi} = n\bar{v}\,\mathrm{Im}\left\langle\sigma^{(\kappa)}_{fi,fi}\right\rangle \quad \text{and} \quad \gamma_{fi} = n\bar{v}\,\mathrm{Re}\left\langle\sigma^{(\kappa)}_{fi,fi}\right\rangle, \quad (2)$$

where n is the number density of the collision partner species, $\bar{v}$ is the average thermal relative collision speed,

$$\langle\sigma\rangle = \int_0^\infty x\,\mathrm{e}^{-x}\sigma(E_k)\mathrm{d}x \quad (3)$$

and $x = E_k/k_BT$.

The S-matrix elements required in Eq. (1) can be obtained by solving the set of close-coupled equations for the radial wave functions [26]

$$\frac{\hbar^2}{2\mu}\left[-\frac{\mathrm{d}^2}{\mathrm{d}R^2}+\frac{l'(l'+1)}{R^2}-k'^2\right]u^{Jvjl}_{v'j'l'}(R) + \sum_{v''j''l''}\langle Jv'j'l'|V|Jv''j''l''\rangle u^{Jvjl}_{v''j''l''}(R) = 0, \quad (4)$$

where μ is the reduced mass of the colliding pair, V is the intermolecular potential, $k\!\setminus\!'$ is the wave vector after collision:

$$k'^2 = \frac{2\mu}{\hbar^2}(E_k+E_{vj}-E_{v'j'}),$$

E_{vj} is the internal vibration–rotation energy of the molecule, and $u^{Jvjl}_{v'j'l'}(R)$ satisfies the asymptotic boundary condition

$$u^{Jvjl}_{v'j'l'}(R) \underset{R\rightarrow\infty}{\sim} \delta_{j'j}\delta_{v'v}\delta_{l'l}\,\mathrm{e}^{-\mathrm{i}(kr-l\pi/2)} - \sqrt{\frac{k}{k'}}S^J_{v'j'l',vjl}\,\mathrm{e}^{\mathrm{i}(k'r-l'\pi/2)}. \quad (5)$$

Numerical values of the S-matrices and the cross sections $\sigma^{(\kappa)}_{f'i',fi}(E_k)$ were computed using the program MOLSCAT [28]. The matrix elements of the XC(fit) potential are decomposed as

$$\langle v'j'l'J|V(R,\theta,\xi)|vjlJ\rangle = \sum_{k\lambda}\langle v'j'|\xi^k|vj\rangle V_{k\lambda}(R)\langle j'l'J|P_\lambda(\cos\theta)|jlJ\rangle, \quad (6)$$

where R is the distance between the Ar atom and the centre-of-mass of the hydrogen molecule, θ is the angle between R and the axis of the molecule, $P_\lambda(\cos\theta)$ is the Legendre polynomial of order λ, and $\xi = (r-r_0)/r_0$ is the diatom stretching coordinate, where r is the hydrogen molecule bond length and r_0 the expectation value of r in the ground vibration–rotation level of H_2. Further details regarding these calculations are presented in Refs. [25,27].

Table 1
Polarized H_2–Ar $Q_1(1)$ shifting and half-width broadening coefficients. Numbers in parentheses are the reported experimental uncertainties in the last digits shown

T (K)	Experiment		Close-coupling theory	
	Ref. [4]	Ref. [8]	Ref. [18]	This work
Shifting coefficients (10^{-3} cm^{-1} amagat^{-1})				
295	−12.0(1)	−11.82(20)	−7.3	−12.22
450	−8.2(1)	−8.35(20)	−1.0	−8.50
596	···	−5.39(25)	···	−5.54
750	−2.7(2)	−3.24(20)	7.9	−3.67
795	···	−2.73(25)	···	−2.08
1000	0.86(40)	0.30(30)	17.2	1.00
Broadening coefficients (10^{-3} cm^{-1} amagat^{-1})				
295	∼4.6	4.42(13)	1.9	1.29
450	···	···	2.8	1.58
596	···	···	···	2.22
700	···	···	5.1	2.91
795	···	···	···	3.72
1000	∼10.0	8.95(20)	8.8	6.04

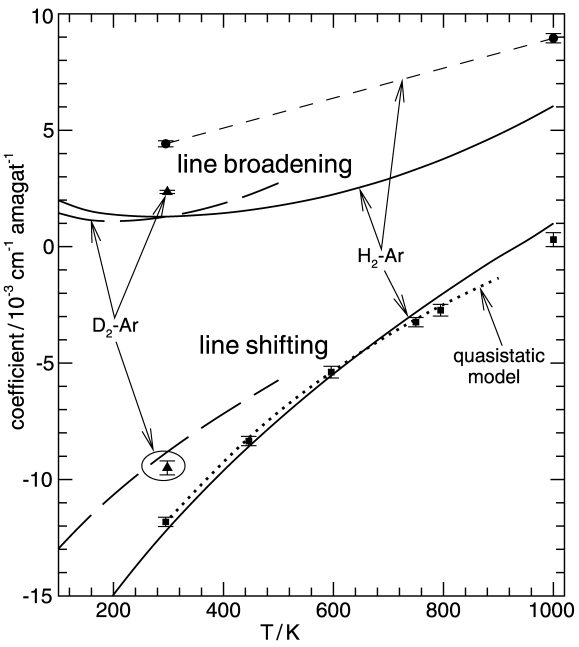

Fig. 1. Polarized $Q_1(1)$ line broadening (positive values) and shifting (negative values) coefficients for H_2–Ar and D_2–Ar (long-dash curves, triangular points): solid curves—present close-coupled values; dotted curve—QS results [12]; points with error bars—experimental values for H_2–Ar from Ref. [8], and for D_2–Ar from Ref. [6] for the shift and Ref. [3] for the width.

3. The polarized Raman $Q_1(1)$ line of H_2–Ar

Experimental line broadening and shifting measurements for the H_2–Ar $Q_1(1)$ line at temperatures between 298 and 1000 K have been reported by Farrow et al. [4] in 1989 and by Berger et al. [8] in 1994. The shifts measured by Berger et al. were the data used by Bissonnette et al. in their determination of the XC(fit) potential [12]. In that work, a simple one-dimensional quasistatic (QS) method was used to simulate the pressure shifting coefficients in the course of the potential optimization, since a full close-coupled calculation would have been far too cumbersome and time-consuming to be incorporated in the iterative multiparameter least-squares fitting procedure. In an attempt to account for errors in the approximate QS method, they adjusted the actual experimental data used in the fit by the differences between the close-coupled results which Green had obtained using the older TT_3 potential energy surface [18] and QS theory values generated for that same potential. The present close-coupled calculations of these shifts on the XC(fit) surface will provide a direct test of the validity of that correction procedure. Berger et al. [8] also reported high-resolution pressure broadening coefficients at 295 and 1000 K, which offer an independent test of the ability of the XC(fit) potential to predict the broadening of Raman Q-lines.

Table 1 lists our close-coupled results for the pressure broadening and shifting coefficients of the polarized H_2–Ar $Q_1(1)$ line, together with the experimental data and the results of Green's calculations using the older TT_3 potential surface. As discussed previously [25], computational errors due to basis size and numerical convergence limitations are estimated to be no more than ca. 1.2%. However, the theoretical predictions above 700 K should be considered somewhat less reliable, since the shifting and broadening cross sections were only calculated for total energies up to $E_k = 2900\ \text{cm}^{-1}$, and were linearly extrapolated to higher energies. This was the highest kinetic energy possible without including another channel in the close-coupled calculation, and is similar to the maximum energy of $E_k = 2500\ \text{cm}^{-1}$ used by Green [18]. However, the extrapolation region contributes 15% of the thermally averaged broadening cross section at 700 K, and 40% at 1000 K. The broadening cross sections are found to

Table 2
Pressure broadening and shifting coefficients for the rotational Raman $S_0(j)$ lines of H_2–Ar

T (K)	Pressure broadening γ_j (MHz m^3 mol^{-1})		Pressure shifting δ_j (MHz m^3 mol^{-1})	
	Theory	Experiment [29]	Theory	Experiment [29]
$j = 0 \rightarrow 2$				
120	0.335	0.44(2)	−0.769	–
123	0.337	–	−0.761	−1.19(4)
181	0.381	0.385(7)	−0.588	–
200	0.416	–	−0.526	−0.48(4)
292	0.684	–	−0.206	−0.16(4)
300	0.714	0.77(2)	−0.177	–
$j = 1 \rightarrow 3$				
120	0.353	0.50(2)	−1.336	–
123	0.350	–	−1.324	−1.22(4)
181	0.341	0.39(3)	−1.107	–
200	0.355	–	−1.038	−0.83(4)
292	0.488	–	−0.697	−0.78(5)
300	0.504	0.59(2)	−0.666	–
$j = 2 \rightarrow 4$				
181	0.267	0.24(4)	−1.833	–
200	0.284	–	−1.761	−1.43(4)
292	0.405	0.49(2)	−1.426	−1.59(5)

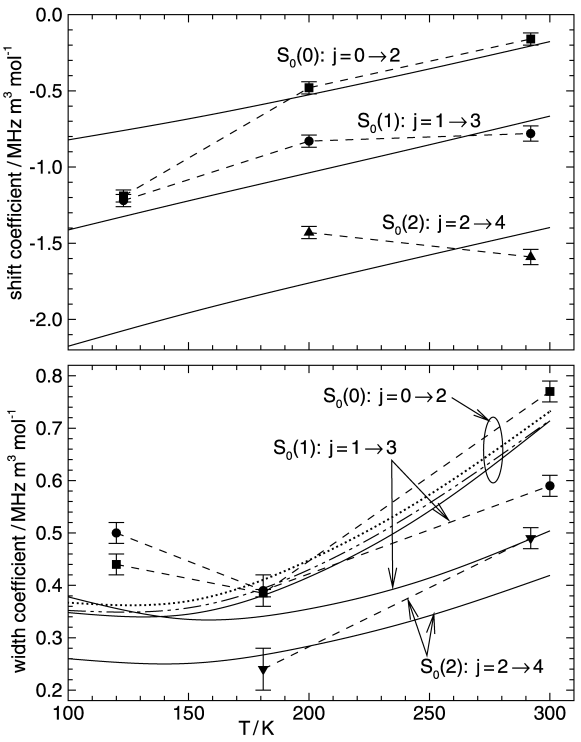

Fig. 2. Comparison of pure rotational Raman $S_0(j)$ broadening and shifting coefficients for H_2–Ar calculated from the XC(fit) potential (solid curves) with experimental data from Ref. [29] (points), and (for $S_0(0)$) also with earlier line shift coefficient predictions [20] based on the $BC_3(6,8)$ (dotted curve) and $TT_3(6,8)$ (dot-dashed curve) potential energy surfaces. Note that 1 MHz m^3 mol^{-1} ≃ 1.49×10^{-3} cm^{-1} amagat^{-1}.

be very close to linear in energy at 2000 cm^{-1}, but the shifting cross sections appear to have a slightly positive second derivative. Thus the linear extrapolation may result in shift predictions which are algebraically slightly smaller (i.e. more negative) than the true shifts. At these high temperatures, collisional vibrational transitions may also begin to contribute significantly.

As far as the pressure shifting coefficients are concerned, the results in Table 1 clearly show that the XC(fit) potential is a substantial improvement over the TT_3 surface used in Green's calculations. This is not too surprising, since these pressure shifting data were used in the fits which determined the XC(fit) potential. However, the good agreement found for our close-coupling results does affirm the validity of the procedure of combining the approximate QS method with adjustments of the input data used in the fitting procedure of Ref. [12]. Moreover, as seen in Fig. 1, from room temperature to ca. 750 K the absolute differences between the exact close-coupling and approximate QS results is no more than 0.4×10^{-3} cm^{-1} amagat^{-1}, which in view of the simplicity of the latter, is surprisingly small.

The line broadening results, on the other hand, are a genuine prediction of the XC(fit) potential, since data of this type were not used in its determination. In this case Table 1 shows that the broadening coefficients generated using the XC(fit) potential are in worse agreement with experiment than are the predictions from the TT_3 potential; similar discrepancies were found for the D_2–Ar system [25], where experimental values are available only at 298 K. This points to an inadequacy of the XC(fit) potential for predicting the pressure broadening of vibrational Raman lines for this system. Fig. 1 shows that at room temperature the line broadening coefficients for the two isotopomers are predicted to be approximately the same, while the magnitude of the line shifting

coefficient for H_2–Ar is substantially larger than that for D_2–Ar. Note that the calculated line broadening coefficients for both isotopomers pass through minima as functions of temperature, the minimum occurring at a slightly lower temperature for D_2–Ar than H_2–Ar. These minima can be attributed to minima in pressure broadening cross sections as a function of collisional kinetic energy [25,27].

4. The pure rotational Raman $S_0(j)$ lines of H_2–Ar

Experimental measurements of pressure broadening and shifting of the pure rotational $S_0(j)$ Raman lines of H_2 in Ar for temperatures 120–300 K have also been reported [29]. These are interesting because with $v_i = v_f = 0$ (Eq. (1)), only purely rotational excitations contribute to the line shape cross sections, so these data are expected to be relatively insensitive to the diatom-stretching dependence of the intermolecular potential. The XC(fit) potential is expected to be accurate in predicting these pure rotational Raman line properties, since the vibrationally averaged potential for $H_2(v = 0)$ with Ar is particularly well probed by the experimental data used in determining the XC(fit) potential.

Table 2 lists the line broadening and shifting coefficients of pure rotational Raman S-branch lines computed using the XC(fit) potential, and compares them with the corresponding experimental values. Fig. 2 presents plots showing the temperature dependence of these results. As in Ref. [25], the accuracy of our computation is expected to be within 1.6%. The S_0-branch broadening and shifting coefficients are smaller in magnitude by a factor of four or more than those for the vibrational Q_1-branch, but the qualitative behaviour is similar. As with the Q_1-branch, the theoretical shifting coefficients decrease in magnitude with temperature in a nearly linear fashion in this temperature range, with similar slopes. However, the experimental values do not show such regular behaviour. The calculated broadening coefficients all pass through minima at temperatures between 130 and 170 K, distinctly lower temperatures than the minima of the H_2–Ar and D_2–Ar $Q_1(1)$ broadening coefficients (see Fig. 1).

Although most of the predicted S_0-branch broadening and shifting coefficients lie outside the reported experimental error bars, the differences are not systematic or as large as in the case of the $Q_1(j)$-branch results. Our theoretical values are generally within 20% of the experimental values, with a maximum difference of 38%. Moreover, the lower segment of Fig. 2 shows that the $S_0(0)$ line broadening coefficients calculated by the close-coupling method using two previous potentials [20] are in good agreement with those obtained here for the XC(fit) potential. This is, perhaps, not surprising, since $v = 0$ pure rotational Raman line broadening is expected to be most sensitive to the regions of the potential energy surface which have been most accurately determined by the discrete IR spectra of Van der Waals complexes and virial coefficient data used to determine those surfaces. On the other hand, those three surfaces do have very different analytic forms, and the fact that their predictions are in such close agreement lends credence to their validity. Thus, it is reasonable to conclude that the pure rotational Raman lineshape parameters calculated from the XC(fit) potential predictions are indeed reliable, and that the apparent discrepancies with experiment seen in Table 2 and Fig. 2 reflect overly optimistic estimation of experimental uncertainties.

5. Effect of modifying the XC(fit) potential energy surface

Fig. 2 shows that the magnitude and temperature dependence of the $S_0(0)$ line broadening coefficient calculated from the XC(fit) potential are very similar to those generated from the earlier TT_3 and $BC_3(6,8)$ surfaces. Since the $S_0(j)$ pure rotational Raman transitions occur entirely within the ground vibrational state of the diatom, this suggests that the large differences between the Q_1-branch line broadening and shifting coefficients calculated from the XC(fit) and TT_3 potential energy surfaces (see Table 1) are due to differences in the diatom bond-length dependence of those surfaces, which make the effective anisotropic potential for $H_2(v = 1)$–Ar different from that for $H_2(v = 0)$–Ar. One reason for these differences will certainly be the fact that the $Q_1(j)$ lineshift data were used in determining the XC(fit) potential, but not the earlier surfaces.

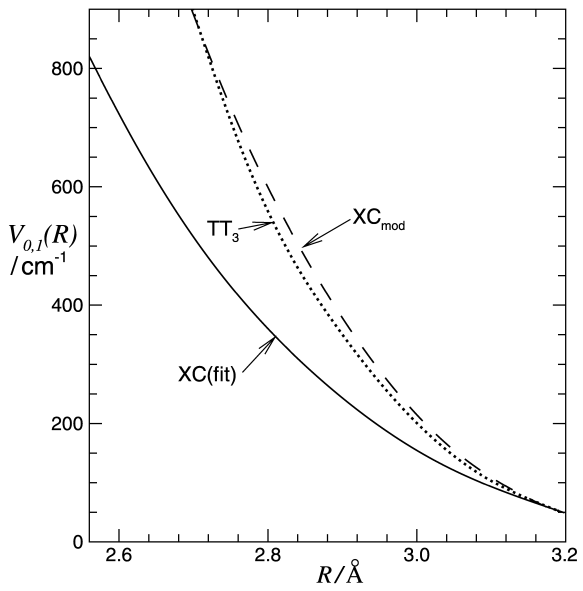

Fig. 3. Isotopic potential stretching dependence functions $V_{0,1}(R)$ for the XC(fit) [12] (solid curve), TT_3 [20] (dotted curve), and present modified XC_{mod} (dashed curve) surfaces.

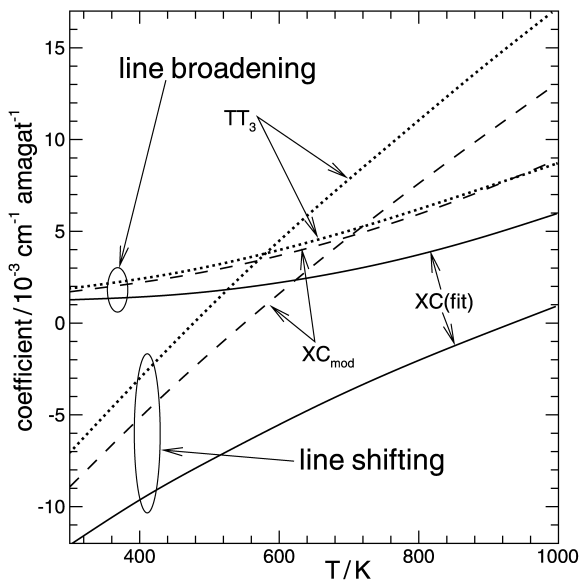

Fig. 4. Pressure broadening and shifting coefficients for the $Q_1(1)$ Raman line of H_2–Ar calculated from the XC(fit) (solid curves), TT_3 (dotted curves), and present modified XC_{mod} (dashed curves) potential surfaces.

In general potential energy surfaces for an atom–diatom system may be expanded in the form

$$V(R,\theta,r)=\sum_{\lambda}\sum_{k}\xi^{k}V_{\lambda,k}(R)P_{\lambda}(\cos\theta). \tag{7}$$

As shown by Figs. 3 and 4 of Ref. [12], the most dramatic differences between the TT_3 and XC(fit) surfaces is in the radial strength functions $V_{0,1}(r)$ and $V_{2,1}(r)$ defining the linear diatom-stretching dependence of the isotropic and leading anisotropy terms in the potential, at small values of the atom–diatom separation coordinate R (at $R \lesssim 3.3$ Å for $V_{0,1}(r)$ and $R \lesssim 4$ Å for $V_{2,1}(r)$). Thus, it seems appropriate to focus on these two components of the potential when trying to understand the discrepancies with experiment.

Some calculations by Green [18] using modifications of the TT_3 potential led him to conclude that the deficiencies of its line shifting and broadening coefficient predictions (see Table 1) were due to deficiencies in its isotropic stretching-dependence radial strength function $V_{0,1}(R)$. In particular, he found that adding a smoothly connected ad hoc quadratic correction to this function for distances $R \leq 3.05$ Å gave changes in the shift cross sections of about the right magnitude and sign to remove the discrepancies of the TT_3 pressure shifting coefficients. Unfortunately, the quality of the experimental $Q_1(1)$ line broadening data available at that time did not allow meaningful tests of that property.

Similar tests performed in this work show that the broadening coefficients are also sensitive to the $V_{0,1}(R)$ part of the potential, and also that changes to the short-range behaviour of the anisotropy stretching-dependence function $V_{2,1}(R)$ mainly affect the shifting coefficients. Fig. 3 compares the short-range behaviour of the $V_{1,0}(R)$ functions for the XC(fit) and the TT_3 potentials with each other and with a modification of the XC(fit) $V_{1,0}(R)$ function, labelled XC_{mod}, which was obtained by adding the quadratic term $\Delta V_a(R)=\alpha_a(R_a-R)^2$ to $V_{1,0}^{XC}(R)$ for $R<R_a$, where $\alpha_a = 1500\,\mathrm{cm}^{-1}/\mathrm{Å}^2$ and $R_a = 3.2$ Å were chosen to make the resulting function similar to the corresponding term in the TT_3 potential. Fig. 4 shows that broadening and shifting coefficients for the H_2–Ar $Q_1(1)$ line calculated using this surface both become similar to the TT_3 predictions, with the agreement being relatively much better for the

broadening coefficients. This does tend to confirm Green's suggestion that the differences in the Raman Q-branch predictions of the XC(fit) potential and the TT_3 potential are largely due to differences in the $V_{10}(R)$ isotropic stretching radial strength function, but it also shows that modifying this function has significant effects on the broadening coefficients. In particular, the more repulsive wall of the TT_3 and XC_{mod} potentials for $H_2(v = 1)$ makes their Q-branch line broadening predictions closer to experiment, while the less repulsive wall of the XC(fit) potential for $H_2(v = 1)$ yields shifting coefficients in better agreement with experiment. However, we were not successful in getting agreement with experiment for both the broadening and shifting coefficients correct simply through ad hoc modifications only to this part of the potential.

In a further study, this same quadratic correction term $\Delta V_a(R)$ was added to the $V_{2,1}(R)$ term of the XC(fit) potential, and close-coupled calculations were performed at a small number of collisional kinetic energies between $E_k = 265$ and 920 cm^{-1}. Compared to the effect of modifying the $V_{0,1}(R)$ term, this produced only ca. 5–10% changes in the shifting cross sections, and less than 2% changes in the broadening cross sections. Moreover, adding this term to the XC(fit) potential $V_{2,1}(R)$ term causes the predicted line shifting coefficients to become more negative, which is in the opposite direction to the effect of increasing the $V_{1,0}(R)$ repulsive wall.

In further testing, the XC(fit) surface $V_{0,1}(R)$ and $V_{2,1}(R)$ functions in the attractive potential well region were modified by adding a term of the form $\alpha_{bc}(R - R_b)(R - R_c)$ on the subinterval $R_b < R < R_c$. The values $R_b = 3.3$ Å, $R_c = 4.1$ Å and $\alpha_{bc} = -20\ cm^{-1}/Å^2$ yield a correction function with an extremum of $-3.2\ cm^{-1}$ at 3.7 Å. Adding this term to the XC(fit) potential $V_{1,0}(R)$ function changed the shifting and broadening cross sections by 5–10%, while application to $V_{2,1}(R)$ changed them by less than 0.5%. Note, however, that while interesting as a model calculation, this type of modification of $V^{XC}_{0,2}(R)$ is physically unrealistic, as it would cause completely unacceptable changes in the discrete infrared spectra. Modifications to the long-range stretching dependence were not considered because the overall interaction is sufficiently weak there that plausible modifications would have negligible effects on the lineshape coefficients.

6. Discussion and conclusions

It is clear that the ad hoc modifications of the XC(fit) potential energy surface described above were not fully successful in getting both the broadening and shifting coefficients for the Q_1-branch transitions to agree with experiment. However, it is interesting to note (see Figs. 3 and 4 in Ref. [12]) that the most dramatic differences between the leading components of the XC(fit) and TT_3 potential energy surfaces were the differences in their short-range stretching dependence of the potential anisotropy, $V_{2,1}(R)$, and that the onset of those differences occurred at the relatively large intermolecular distance of 4 Å. Thus, it may be that the correction function $\Delta V_a(R)$ considered above is too modest a change as far as $V_{2,1}(R)$ is concerned.

Perhaps the most interesting feature of the present results is their demonstration that changes to the short-range behaviour of $V_{0,1}(R)$ significantly affects *both* broadening and shifting coefficients, while modifications to $V_{2,1}(R)$ mainly affect the latter. Although the QS model for predicting the shifting coefficients used in the analysis of Ref. [12] could in principle take account of diatom stretching-dependence of the potential anisotropy, that analysis used a strictly one-dimensional QS simulation, and hence attributed the pressure shifting coefficients solely to the stretching dependence of the isotropic potential. The present work shows that this was not correct. Moreover, since modification of $V_{2,1}(R)$ mainly affects the shifting coefficients, it seems likely that a resolution of the discrepancies for the lineshape coefficients of the XC(fit) potential could be achieved by correlated modifications of the short-range behaviour of both $V_{0,1}(R)$ and $V_{2,1}(R)$.

Acknowledgments

We thank Professor William J. Meath, whose fundamental contributions to theoretical chemical physics have been so important to the field, and whose generosity and friendship have so enriched our lives. We also thank Professor F.R.W. McCourt for

many helpful discussions. This work is supported in part by the Natural Sciences and Engineering Research Council (NSERC) of Canada.

References

[1] R. Shafer, R.G. Gordon, J. Chem. Phys. 58 (1973) 5422.
[2] H. Rabitz, Annu. Rev. Phys. Chem. 25 (1974) 155.
[3] K.C. Smyth, G.J. Rosasco, W.S. Hurst, J. Chem. Phys. 87 (1987) 1001.
[4] R.L. Farrow, L.A. Rahn, G.O. Sitz, G.J. Rosasco, Phys. Rev. Lett. 63 (1989) 746.
[5] J.W. Forsman, P.M. Sinclair, P. Duggan, J.R. Drummond, A.D. May, Can. J. Phys. 69 (1991) 558.
[6] G.J. Rosasco, W.J. Bowers Jr., W.S. Hurst, J.P. Looney, K.C. Smyth, A.D. May, J. Chem. Phys. 94 (1991) 7625.
[7] P.M. Sinclair, J.W. Forsman, J.R. Drummond, A.D. May, Phys. Rev. A 48 (1993) 3030.
[8] J.P. Berger, R. Saint-Loup, H. Berger, I. Bonamy, D. Robert, Phys. Rev. A 49 (1994) 3396.
[9] P.M. Sinclair, P. Duggan, M. Le Flohic, J.W. Forsman, J.R. Drummond, A.D. May, Can. J. Phys. 72 (1994) 885.
[10] P.M. Sinclair, P. Duggan, J.W. Forsman, J.R. Drummond, A.D. May, Can. J. Phys. 72 (1994) 891.
[11] P.M. Sinclair, P. Duggan, J.R. Drummond, A.D. May, Can. J. Phys. 73 (1995) 530.
[12] C. Bissonnette, C.E. Chuaqui, K.G. Crowell, R.J. Le Roy, J. Chem. Phys. 105 (1996) 2639.
[13] W. Meyer, P.C. Hariharan, W. Kutzelnigg, J. Chem. Phys. 73 (1980) 1880.
[14] R. Blackmore, S. Green, L. Monchick, J. Chem. Phys. 88 (1988) 4113.
[15] S. Green, R. Blackmore, L. Monchick, J. Chem. Phys. 91 (1989) 52.
[16] R. Brezina, W.-K. Liu, S. Green, Phys. Rev. A 51 (1995) 3645.
[17] R. Brezina, S.H. Lin, W.-K. Liu, Chem. Phys. Lett. 262 (1996) 437.
[18] S. Green, J. Chem. Phys. 93 (1990) 1496.
[19] R.J. Le Roy, J.M. Hutson, J. Chem. Phys. 86 (1987) 837.
[20] J.M. Hutson, J. Chem. Phys. 86 (1987) 854.
[21] K.-C. Ng, W.J. Meath, A.R. Allnatt, Chem. Phys. 32 (1978) 175.
[22] K.-C. Ng, W.J. Meath, A.R. Allnatt, Chem. Phys. 37 (1979) 237.
[23] W.J. Meath, D.J. Margoliash, B.L. Jhanwar, A. Koide, D.G. Zeiss, in: B. Pullman (Ed.), Proceedings of the 14th Jerusalem Symposium on Quantum Chemistry and Biochemistry, Reidel, Dordrecht, 1981, pp. 101–115.
[24] H. Sabzyan, W.P. Power, F.R.W. McCourt, J. Chem. Phys. 108 (1998) 2361.
[25] L. Waldron, W.-K. Liu, J. Chin. Chem. Soc. 48 (2001) 439.
[26] W.-K. Liu, Quantum theory of inelastic scattering, in: S. Wilson (Ed.), Handbook of Molecular Physics and Quantum Chemistry, Part 18, vol. III, Wiley, Chichester, 2002, Chapter 3.
[27] L. Waldron, Quantal calculation of Raman lineshape parameters for H_2 and D_2 in Ar, MSc thesis, The University of Waterloo, 1998.
[28] J.M. Hutson, S. Green, MOLSCAT Computer Code, Version 14, distributed by Collaborative Computational Project No. 6 of the Science and Engineering Research Council, UK, 1994.
[29] P.W. Hermans, A. van Die, H.F.P. Knaap, J.J.M. Beenakker, Physica 132A (1985) 233.